A New Aspect for the Insertion of the 16-Electron Species (η^5-C_5H_5)ML into Saturated Hydrocarbons. A (η^5-C_5H_5)ML + CH_4 (M = Rh, Ir; L = CO, SH_2, PH_3) Case Study†

Ming-Der Su* and San-Yan Chu*

Department of Chemistry, National Tsing Hua University, Hsinchu 30043, Taiwan, ROC

Received: December 16, 1996; In Final Form: April 14, 1997⊗

The potential energy surfaces of the oxidative addition reaction CpML + CH_4 → CpML(H)(CH_3) (Cp = η^5-C_5H_5; M = Rh, Ir; L = CO, PH_3, SH_2) have been studied at the MP2/LANL1DZ and MP4SDTQ/LANL2DZ//MP2/LANL1DZ levels of theory. It has been found that there should be two competing pathways in those reactions, which can be classified as a σ or π approach, with the former being more favorable. A qualitative model which is based on the theory of Pross and Shaik (Su, M.-D. *Inorg. Chem.* **1995**, *34*, 3829) has been used to develop an explanation for the barrier heights. As a result, our theoretical findings suggest that the singlet−triplet splitting ($\Delta E_{st} = E_{triplet} - E_{singlet}$) of the CpML (M = Rh, Ir) species can be a guide to predict its reaction activity for oxidative additions. Considering the substituent effect and the nature of the metal center, the following conclusions therefore emerge: for the 16-electron CpML complex, a stronger electron-donating ligand as well as a heavier transition-metal center (such as Ir) will result in a smaller ΔE_{st} and, in turn, will be a potential model for the oxidative addition of saturated C−H bonds. Conversely, a better electron-withdrawing ligand as well as a lighter transition-metal center (such as Rh) will lead to a larger ΔE_{st} and then will be a good model for reductive coupling of C−H bonds. The results obtained are in good agreement with the available experimental results and allow a number of predictions to be made.

I. Introduction

Considerable attention has been paid during the past decade to studying the special reactivity of C−H bond activation systems and the ability of transition-metal complexes to insert into saturated carbon centers under relatively mild homogeneous conditions.[1] Among organometallic systems, there has been much interest in the chemistry of Cp*ML_2 and Cp*MLH_2, (Cp* = η^5-C_5Me_5; M = Rh, Ir; L = CO, PR_3, C_2H_4), as these complexes produce a postulated unsaturated intermediate Cp*ML upon light irradiation.[2−4] The reactive 16-electron metal center in this intermediate then undergoes oxidative addition to the C−H bond of a solvent molecule. Thus, it is important to learn the chemical requirements behind such C−H bond activations and their mechanisms. On a more practical level, such information should help to develop methods for converting saturated hydrocarbons, such as those found in petroleum and formed in Fischer−Tropsch reactions, into functionalized compounds more easily utilized in chemical conversions. It is therefore not surprising that much experimental and theoretical work has been devoted to the study of the bonding nature and energy sequence of such C−H bond activation reactions. Most of the effort, however, has been directed to the problem of photochemical reactivity in those types of molecules, the key reaction intermediates involved in the mechanism, and the potential energy surfaces of the oxidative addition reaction of the X−H bond (X = H, C, Si, N, O), etc.

The present work will not address the aforementioned problems but will rather consider the following: the effect of the substituent for the ancillary ligand L as well as the central metal M in the coordinatively unsaturated 16-electron CpML complex. To our knowledge, there is no systematic ab initio study for the substituent effect on the CpML systems. Therefore, the purpose of this work is to explain the trend of the reactivities in numerous variations in the metal and ligands and to bring out the determined factor that controls the activation barrier for the CpML reactions. Despite the numerous theoretical studies in the C−H activation area,[4] we believe that a somewhat different approach and some new aspects emphasized here may supplement their results. It will be shown that the reaction activity of the 16-electron CpML complex correlates nicely with its singlet−triplet splitting. Namely, one may expect the singlet−triplet splitting of the 16-electron CpML (M = Rh, Ir) species to be a guide to predict its activity for oxidative addition reactions.

II. Electronic Structure of the CpML + CH_4 Model System

To highlight the questions which formed the basis for our study, it is perhaps worthwhile to review briefly the electronic structure of the CpML fragment. A general outline of the valence molecular orbitals (MOs) in CpML has been given previously,[5,6] which are explicitly shown in Figure 1. They are identified as 1a′, 1a″, 2a′, 2a″, and 3a′ orbitals under C_s symmetry. Basically, the former three orbitals (1a′, 1a″, and 2a′) have more or less bonding interactions between the central metal M and the ancillary ligand L so that they all lie in lower energy. At the highest energy are the two metal-based orbitals, 2a″ and 3a′, composed primarily of d_{yz} and d_{xz} orbitals, respectively. Both are destabilized by interaction with occupied π orbitals on the Cp ring, and 3a′ of the highest energy is, in addition, destabilized by the σ orbital on L. Moreover, it has to be pointed out that the LUMO 3a′ is a hybridized orbital, since some metal s and p characters are mixed into d_{xz} orbitals as schematically indicated in **1**. Thus, this resultant MO, the σ acceptor level of bent CpML, is heavily weighted on the metal and is nicely hybridized toward the missing ligand of a parent $CpML_2$ complex.[6]

† This article is dedicated to Professor Yuan T. Lee on the occasion of his 60th birthday.

⊗ Abstract published in *Advance ACS Abstracts,* July 1, 1997.

S1089-5639(97)00021-2 CCC: $14.00

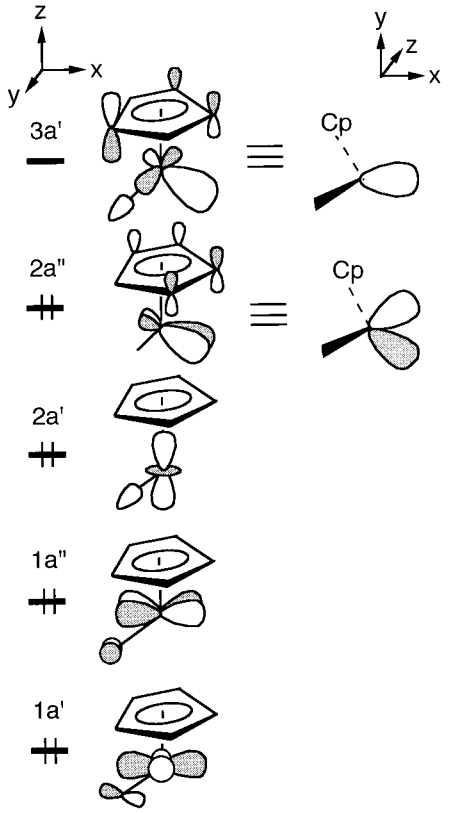

Figure 1. Valence molecular orbitals of the 16-electron CpML complex.

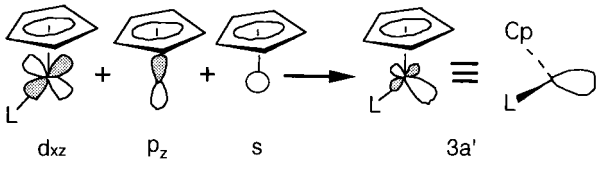

1

Furthermore, it is also worthwhile to briefly describe a frontier molecular orbital (FMO) model, based on a set of fragment MOs, which has been proved to be a good approach that allows one to predict the approximate reaction trajectory and transition-state structure for the insertion of the electrophile into the saturated C−H bonds. It must be pointed out that this concept of insertion mechanism was expressed for the first time by Bach et al.[7] In a canonical MO description of a hydrocarbon, there are no isolated MOs that describe a particular C−H σ bond. For example, in methane, there is a lower lying $2A_1$ orbital and three degenerate T_2 orbitals.[8] In a tetrahedral array, both hydrogens (or carbons) directly bound to the sp^3 carbon occupy a common plane, and they are related by symmetry and may comprise an orbital with σ symmetry (σ_{CH_2}) as in **2** or a π_{CH_2} orbital as in **3**.[9] Moreover, since CH_2 and 16-electron CpML

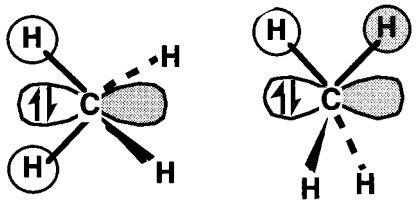

2 **3**

are isolobal,[10] then each should have two valence orbitals with the same symmetry properties (for CpML, see Figure 1). These are shown in **4**, in which each fragment has one orbital of a′ and a″ symmetry. Note that the energy ordering in the metal

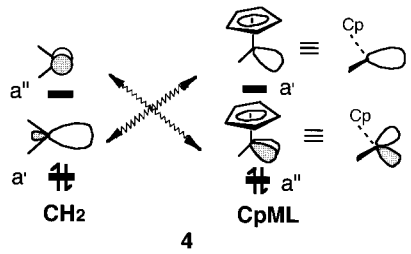

4

fragment differs from that in the carbene. This is a natural consequence of the fact that in CpML, the major contribution to the a″ orbital is the metal d character, while in the a′ orbital, it is a hybrid of metal s, p, and d characters as shown in **1**. Therefore, for a singlet CH_2 fragment, one would assign the two electrons to the a′ orbital, while for a singlet 16-electron CpML species, the two electrons would go into the a″ level. In other words, the frontier orbitals of the 16-electron CpML complex consist of an empty s/p/d hybrid orbital and a d orbital that has a single lone pair of electrons (*vide infra*). It is noteworthy that in the latter orbital (2a″), the d lobe is on the plane which is perpendicular to the "X−M−L" plane (X = the center of the Cp ring).

Therefore, we prefer to use a canonical MO rather than take a localized description of the C−H bond, since it is easier to visualize the coalescence of the electron donor and acceptor when the approximate axis of the reaction is clearly defined. In this qualitative theoretical treatment, we identify the organotransition-metal fragment CpML as having an empty electrophilic orbital (i.e., 3a′ as shown in Figure 1 or 4) that can interact with a filled hydrocarbon fragment orbital that can serve as the terminus for a concerted 1,2-hydrogen migration. Hence, the implication of a σ_{CH_2} (**2**) or a π_{CH_2} (**3**) fragment orbital in methane identifies a molecular plane that is approached by CpML and provides an estimate of the starting geometry to search for a saddle point. See Figure 2. For the σ attack, the 3a′ orbital of CpML overlaps with a hydrocarbon fragment along the axis of its filled atomic p orbital and a 1,2-hydrogen migration to the adjacent pair of electrons (2a″) takes place in concert with C−M bond formation. On the other hand, the π attack proceeds by attack of a filled π_{CH_2} fragment orbital along the axis of the empty s/p/d orbital of the CpML with a concerted hydrogen migration into the CpML lone pair. As a result, the net molecular event involved in the insertion of the CpML complex into a C−H σ bond of methane is the formation of a new metal−carbon σ bond as well as a new metal−hydrogen σ bond, accompanied by the breaking of the C−H σ bond. This is a typical example for the oxidative addition reaction of a transition-metal complex into the C−H bond.[1] In addition, since the experimental evidence suggests that radical intermediates were not involved in the C−H activation reaction for the d^8-CpML systems,[1b,c] it is therefore reasonable to conclude that the mechanism depicted in Figure 2 should be the most likely pathway for 16-electron CpML analogues. We shall see the calculational results supporting this prediction below.

III. Computational Methods

The geometries of the reactants, precursor complexes, transition states, and products were fully optimized by employing the second-order Møller−Plesset (MP2) perturbation theory without imposing any symmetry constraints. All electrons, for which the MOs are described by basis functions, were correlated. For triplet CpML systems, we also carried out the second-order

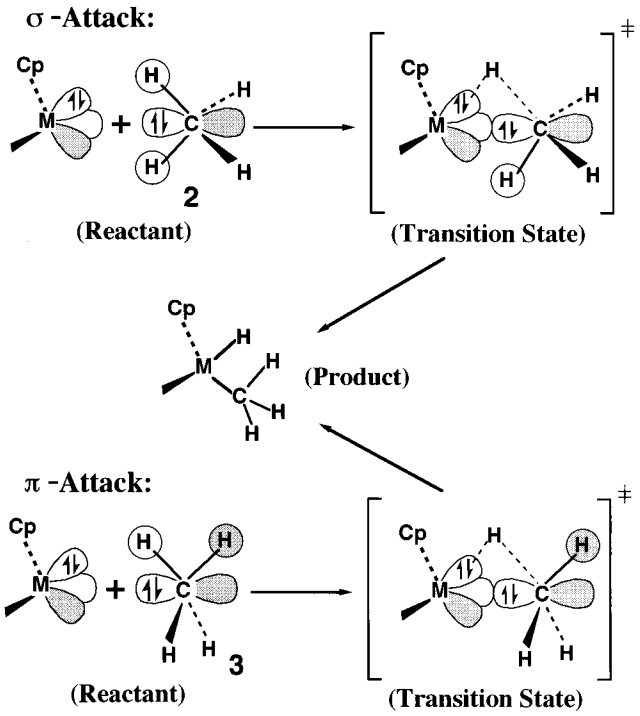

Figure 2. Insertion of CpML into hydrocarbons proceeding along a σ_{CH_2} path, where the empty CpML s/p/d orbital is aligned with the carbon p orbital of a σ_{CH_2} fragment orbital, or along a π_{CH_2} path, where the CpML s/p/d orbital is aligned with a π_{CH_2} fragment orbital.

unrestricted MP calculations (UMP2) with annihilation of the spin contaminants (PUMP2).[11]

The LANL1DZ and LANL2DZ basis sets which contain pseudopotentials for the core electrons and a double-ζ set for valence electrons[12−15] have been used in this study. The LANL2DZ basis differs from the LANL1DZ basis by inclusion of the $(n-1)$s and $(n-1)$p electrons in the valence space of the transition-metal atom. Hence, the MP2 calculation is denoted by MP2/LANL1DZ. Vibrational frequencies at stationary points were calculated at the MP2/LANL1DZ level of theory to identify them as minima (zero imaginary frequencies) or transition states (one imaginary frequency).

For better energetics, single-point calculations with MP2/LANL1DZ geometries were carried out at a higher level of theory; the fourth-order MP level including single, double, triple, and quadruple configurations (MP4SDTQ) was included using the same basis sets as mentioned above, MP4SDTQ/LANL2DZ//MP2/LANL1DZ. Moreover, for triplet CpML, the spin-projected MP perturbation theory to the fourth order (PMP4) with the LANL2DZ basis set was used.[11] All calculations were performed with the Gaussian 92 program.[16]

IV. Results and Discussion

1. Geometries and Energetics of CpML + CH_4. The fully optimized geometries of the reactants, precursor complexes, transition states, and products for CpRhL and CpIrL (L = CO, SH_2, PH_3) calculated at the MP2/LANL1DZ level are given in Figures 3−8, respectively. Also, their energy parameters at the MP2/LANL1DZ and MP4SDTQ/LANL2DZ//MP2/LANL1DZ levels are summarized in Table 1.[17]

Seven interesting results can be drawn from those figures and that table. First, it is clear from Figure 1 that in the triplet state, one electron is situated in the 3a′ orbital, in which antibonding interactions exist between the metal and the ligand as well as the Cp ring, whereas this orbital is empty in the singlet state. The distance r(M−X) between the metal atom and the

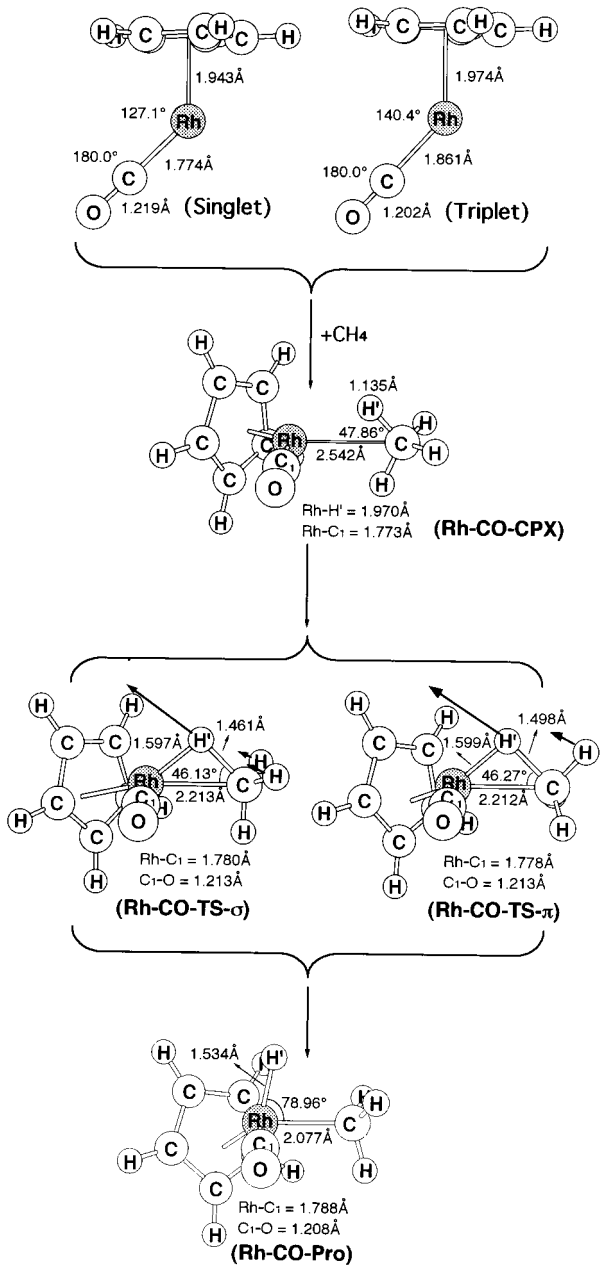

Figure 3. MP2/LANL1DZ-optimized geometries for the reactants (singlet and triplet), precursor complexes, transition states, and products of CpRh(CO). The heavy arrows indicate transition vectors for the single imaginary frequency.

center, X, of the Cp ring, the distance r(M−L), and the angle ∠X−M−L are therefore expected to be larger for the triplet compared to the singlet. This prediction qualitatively agrees with our MP2/LANL1DZ results for all cases as given in Figures 3−8.

Second, according to our MPn calculations in Table 1, it is intriguing to find that the ground state of the fragment is singlet, whereas other complexes are triplets. This implies that a complex with the triplet ground state might insert into the saturated C−H bond via a diradical type of mechanism. Nevertheless, it is well-established that whenever a reactant contains a heavy atom center which is not necessarily directly involved in the reaction, a strong spin−orbit coupling (SOC) may obtain.[18] In other words, a triplet reactant, via the agency of the heavy atom, can provide a spin-inversion process for transferring to the singlet reactant and then undergoing the singlet reaction. Additionally, our MPn results in Table 1 also suggested that those fragments with the triplet ground state

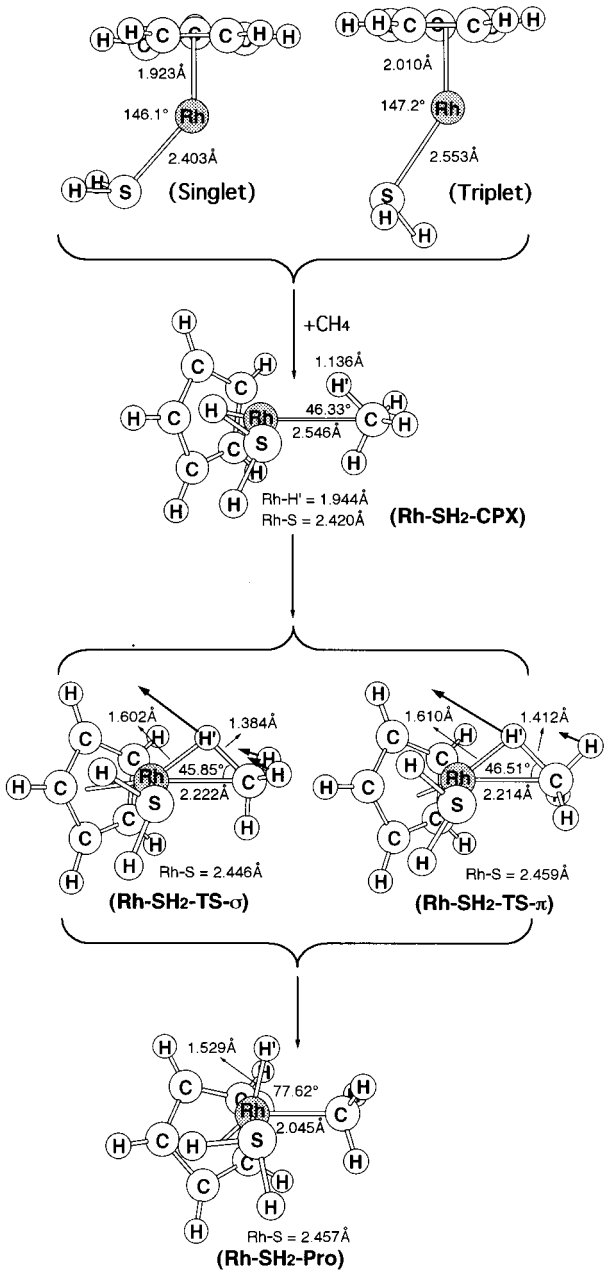

Figure 4. MP2/LANL1DZ-optimized geometries for the reactants (singlet and triplet), precursor complexes, transition states, and products of $CpRh(SH_2)$. The heavy arrows indicate transition vectors for the single imaginary frequency.

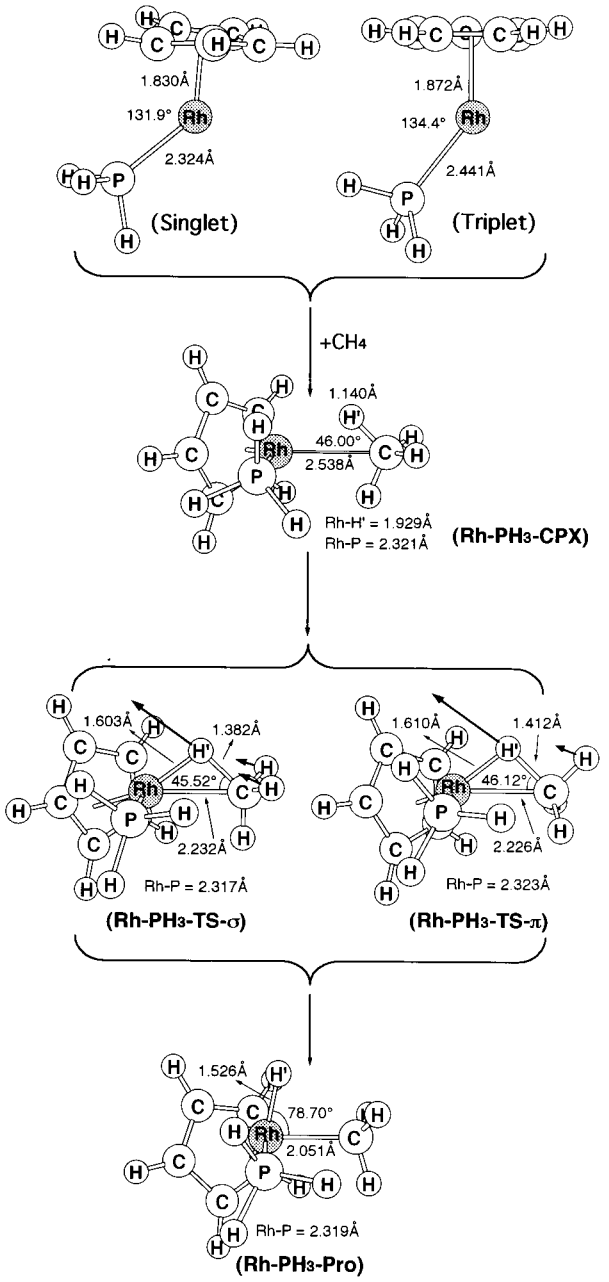

Figure 5. MP2/LANL1DZ-optimized geometries for the reactants (singlet and triplet), precursor complexes, transition states, and products of $CpRh(PH_3)$. The heavy arrows indicate transition vectors for the single imaginary frequency.

would have small excitation energy to the first singlet state; i.e., $\Delta E_{st} = -20$ to -1.1 kcal/mol. Thus, due to the fact that CpML has a small singlet−triplet splitting ΔE_{st} and a heavier transition metal involved, the SOC is expected to be substantial in those oxidative additions and would wash out differentials based on singlet, triplet distinctions. Moreover, as mentioned previously, no radical components have been detected experimentally in the oxidative addition reactions of the 16-electron CpML (M = Rh, Ir) systems. For these reasons, it could well be that our concern about the possible *presence* of reactive singlets and triplets is unnecessary.

Third, as seen in Table 1, the singlet−triplet splitting ΔE_{st} ($=E_{triplet} - E_{singlet}$) of the CpRhL systems is larger than that of the CpIrL systems for each ancillary ligand L. An important origin for such energy differences of spin states of the CpML systems, which has been discussed by Siegbahn,[4e] can be traced to a difference already found for the isolated atoms. Siegbahn pointed out that the rhodium atom has a quartet d^8s^1 ground state with a quite low excitation energy of only 7.8 kcal/mol to the doublet d^9 state, whereas for the iridium atom, the ground state is again a quartet d^7s^2 state but with a high excitation energy to the doublet d^9 state of 60.7 kcal/mol. Moreover, since the CO group is a well-known good π acceptor, it is not surprising that the ΔE_{st} of the CpRh(CO) and CpIr(CO) reactants is larger than that of other CpRhL and CpIrL (L = PH_3, SH_2) systems, respectively. Consequently, one may predict that in the 16-electron CpML systems, a stronger electron-acceptor ligand L should result in a larger singlet−triplet splitting ΔE_{st} ($=E_{triplet} - E_{singlet}$), while a better electron-donor ligand L should lead to a smaller ΔE_{st}.[19,20] This prediction is based on the assumption that the central metal M holds constant, and we shall use this prediction after presenting our other calculational results.

Fourth, as shown in Figures 3−8, both π_{CH_2} and σ_{CH_2} approaches can lead to a first-order saddle point, as determined by the frequency calculations at the MP2/LANL1DZ level. Examination of the single imaginary frequency for each

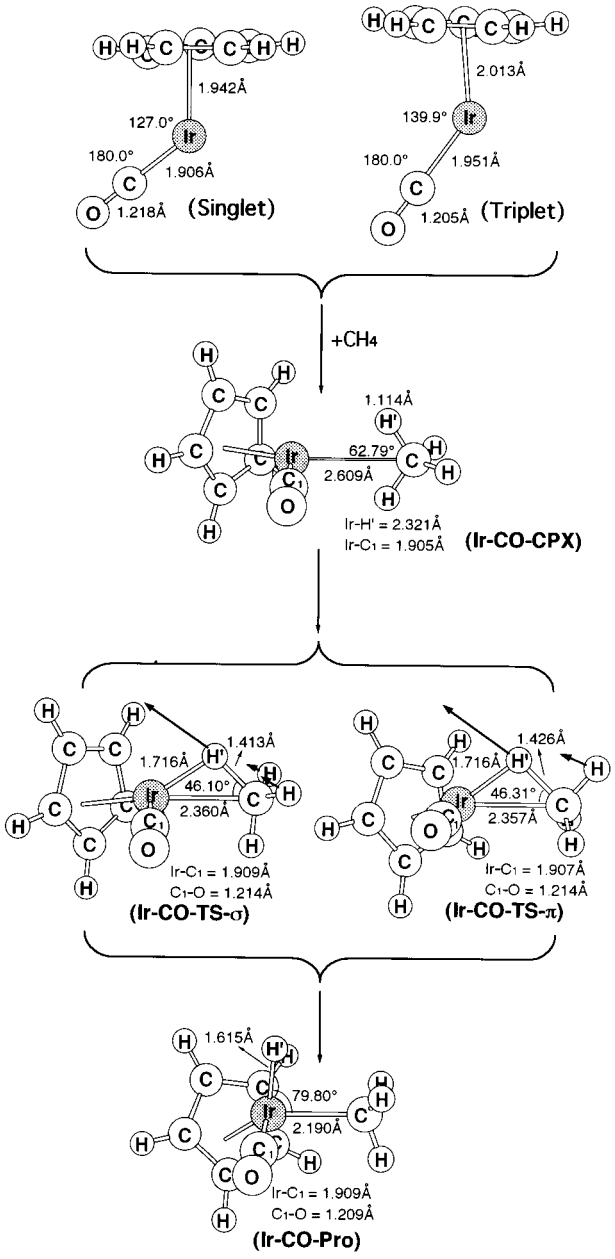

Figure 6. MP2/LANL1DZ-optimized geometries for the reactants (singlet and triplet), precursor complexes, transition states, and products of CpIr(CO). The heavy arrows indicate transition vectors for the single imaginary frequency.

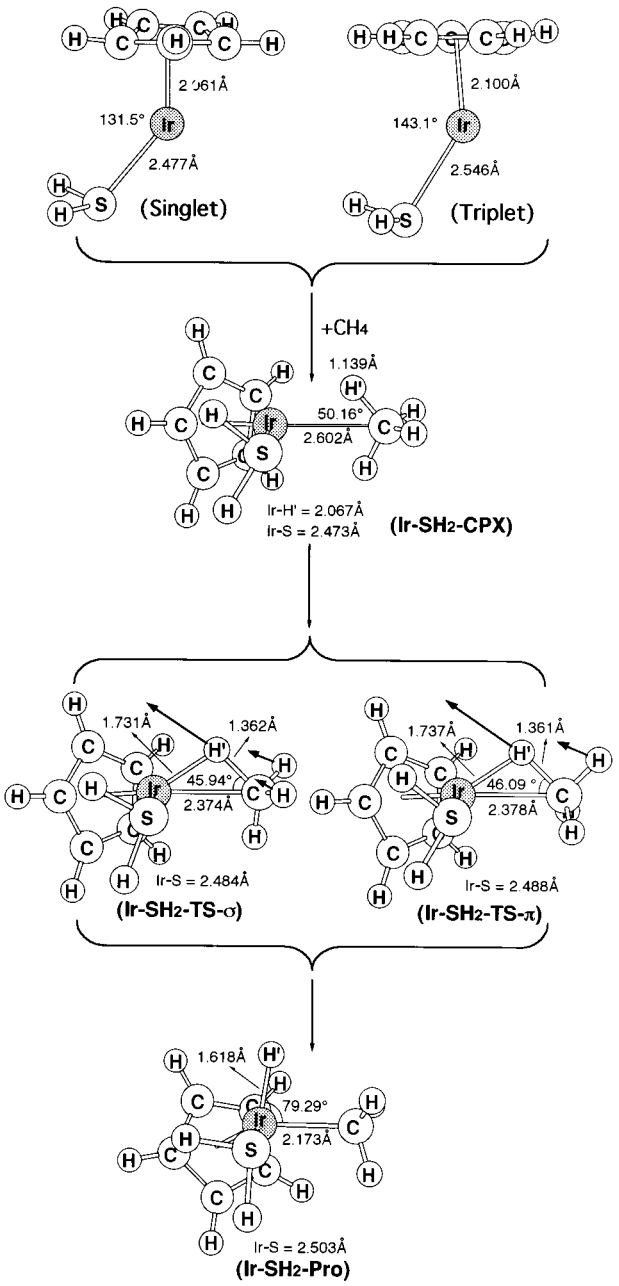

Figure 7. MP2/LANL1DZ-optimized geometries for the reactants (singlet and triplet), precursor complexes, transition states, and products of CpIr(SH_2). The heavy arrows indicate transition vectors for the single imaginary frequency.

oxidative addition reaction provides excellent confirmation of the above prediction where CpML attacks the π_{CH_2} and σ_{CH_2} fragment orbitals along the axis of the central metal s/p/d hybrid orbital. The reaction vectors are all in accordance with the insertion process, primarily the C−H bond stretching with a hydrogen migrating to the metal center.

Fifth, perhaps the primary similarity among those transition states observed for CpRhL and CpIrL at the various ligands (L = CO, PH_3, SH_2) is, as expected earlier, the three-center pattern involving the metal center and carbon and hydrogen atoms undergoing bond cleavage. It is noted that such characteristic three-center transition states are in accordance with the mechanisms postulated by Bergman and Janowicz[2e] and Jones and Feher.[2i]

Sixth, comparing the σ attack and the π attack in Figure 2, one can readily anticipate that the CpML insertion in the σ_{CH_2} orientation has fewer steric interactions than a π_{CH_2} approach and provides the insertion product in its staggered lower energy conformation. This prediction is confirmed by our calculational results as given in Table 1. For instance, the activation barrier of the σ_{CH_2} approach is lower in energy than that of the π_{CH_2} insertion by about 1.2−0.3 kcal/mol at the MP4SDTQ level of theory. Although the energy differences between the σ_{CH_2} and π_{CH_2} approaches to methane are relatively small, in each case the orientation of the lone pair and empty s/p/d hybrid orbital on the metal center is consistent with the basic concepts outlined in this FMO model, Figure 2.

Seventh, examining those conformations of products as shown in Figures 3−8, it is obvious that the methane fragment (H′---CH_3) is poised in a σ_{CH_2} fashion, which is consistent with the above findings for the transition states where the σ_{CH_2} orientation was slightly favored over the π_{CH_2} approach.

2. Discussion of the Potential Energy Surfaces. Since the energetics at the MP2/LANL1DZ level are very similar to those at the MP4SDTQ/LANL2DZ//MP2/LANL1DZ level in the

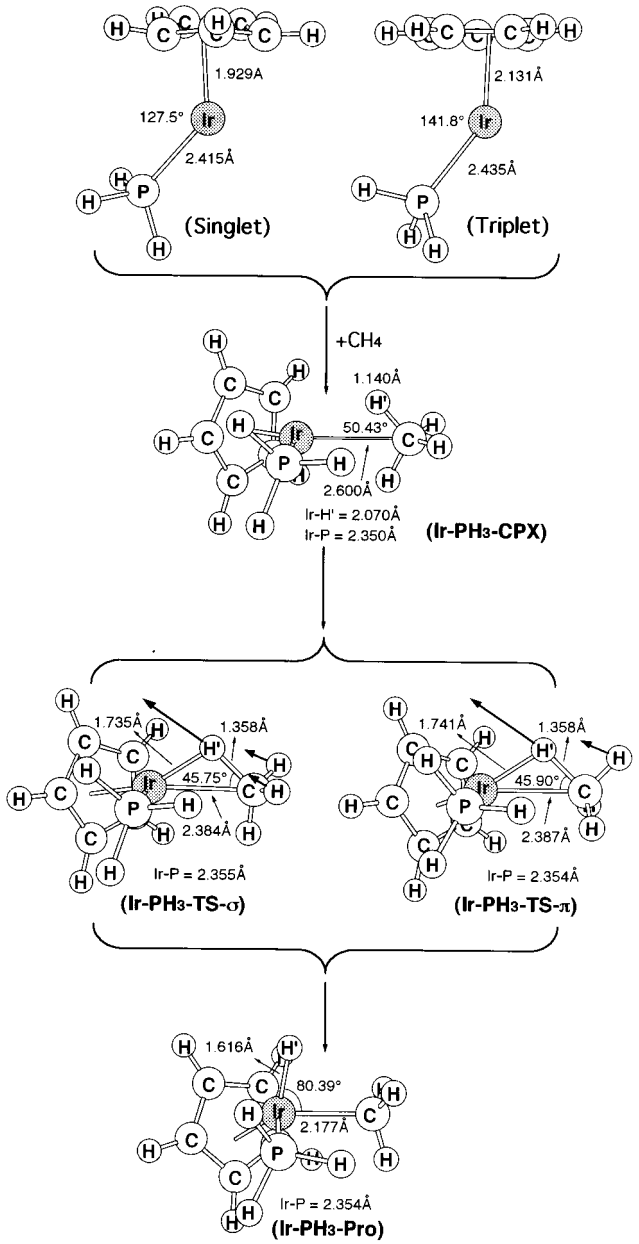

Figure 8. MP2/LANL1DZ-optimized geometries for the reactants (singlet and triplet), precursor complexes, transition states, and products of $CpIr(PH_3)$. The heavy arrows indicate transition vectors for the single imaginary frequency.

activation C−H bond for each system, the potential energy profiles for the latter are therefore summarized in Figure 9.

Three important conclusions can be drawn from Figure 9. First, our model systems have shown that those oxidative addition reactions all proceed in a *concerted* fashion via a three-center transition state in either the σ-attack case or the π-attack case as shown in Figures 3−8, and all lead to the exothermic reactions. The transition-state studies, demonstrating that radical intermediates should not be involved in the C−H activation reaction for 16-electron CpML systems, are consistent with the FMO model (Figure 2) as well as experimental observations.[1c,2e] In addition, it must be mentioned once more that, according to the FMO model, such an oxidative addition to a saturated C−H bond is capable of generating stereoisomers due to the fact that the transition metal is a chiral center. Unfortunately, there are no available structural experimental data to support this prediction.[2e,1,3u]

Second, consider the substituent effect. It is clearly seen that *the more strongly electron-donating the ligand L, the lower the activation energy for oxidative addition (left to right in Figure 9) but also the higher the heat of reductive elimination (right to left in Figure 9).* In addition, *the Ir reactions are more exothermic than their Rh counterparts.* For instance, as demonstrated in Table 1, since the electron-donating ability is in the order $PH_3 > SH_2 > CO$,[21] the barrier height for CH_4 activation with the Rh metal increases in the order $CpRh(PH_3)$ (6.21 kcal/mol) < $CpRh(SH_2)$ (7.33 kcal/mol) < CpRh(CO) (10.3 kcal/mol) and for the Ir metal $CpIr(PH_3)$ (−2.24 kcal/mol) < $CpIr(SH_2)$ (−1.37 kcal/mol) < CpIr(CO) (−0.624 kcal/mol), while the activation energy for CH_4 elimination decreases in the order $CpRh(PH_3)$ (13.0 kcal/mol) ∼ $CpRh(SH_2)$ (13.0 kcal/mol) > CpRh(CO) (8.52 kcal/mol) and $CpIr(PH_3)$ (29.7 kcal/mol) > $CpIr(SH_2)$ (29.5 kcal/mol) > CpIr(CO) (23.5 kcal/mol). Likewise, the exothermicity for oxidative addition increases in the order $CpRh(PH_3)$ (−20.0 kcal/mol) < $CpRh(SH_2)$ (−18.0 kcal/mol) < CpRh(CO) (−11.9 kcal/mol) and $CpIr(PH_3)$ (−46.3 kcal/mol) < $CpIr(SH_2)$ (−43.8 kcal/mol) < CpIr(CO) (−40.5 kcal/mol). From the analysis of these data, it is crucial to find that the electron density at the reacting metal center must play an important role in the C−H oxidative additions, since it is shown that an electron-rich metal center can result in a lower activation energy as well as a higher exothermicity for the C−H activation of methane. These results are also consistent with the prediction that the activation barrier should be correlated to the exothermicity for oxidative additions.[22] Moreover, it is apparent that the difference in reactivity toward hydrocarbons among those fragments CpML (L = CO, PH_3, SH_2) should arise from their electronic factors but not the steric effects of a phosphine ligand compared to a carbonyl, which could prevent the approach of a saturated C−H bond.

Third, our model calculations suggest that *the oxidative additions of a third-row transition metal (such as Ir) should be preferable to those of a second-row transition metal (such as Rh)* since it is demonstrated not only that the former are thermodynamically favorable but also that the kinetic barriers associated with them are typically small. This prediction has been confirmed by many available experimental works.[1b,c,l,p] On the other hand, *the reductive elimination of the second-row metal is more favorable than that of the third-row homologue.* To our knowledge, the experimentally supporting evidence comes from the fact that, in comparison of oxidative additions of the iridium and rhodium intermediates to alkane C−H bonds, the products formed in the latter case are much less stable and undergo reductive elimination at −20 °C.[1b,2b,g] This strongly suggests that the stable oxidative addition products with alkanes will be found predominantly in the third row.

3. Origin of the Barrier for Oxidative Addition of CpML. In this section, we shall use a simple valence-bond model to develop an explanation for the barrier heights discussed above.

According to Su's study[23] based upon the configuration mixing (CM) model described by Pross and Shaik,[24] it was suggested that the singlet−triplet splitting of carbene plays a crucial role in insertion reactions; i.e., the relative stabilities of the lowest singlet and triplet states are in turn a sensitive function of the barrier height for carbenic reactivity. Since, as stated above, 16-electron CpML is isolobal to CH_2,[10] one may envision that these predictions for carbenic reactivity should also apply to the 16-electron CpML systems. We therefore take the oxidative addition reaction CpML + CH_4 as an example by using the CM model as shown in Figure 10 to understand the origin of barrier height and bonding nature of the CpML species.

In the oxidative addition reaction, it may exist in a number of predetermined states, each of which may be approximated

TABLE 1: Energies for Singlet and Triplet CpML Fragments and for the Process CH_4 + CpML → Precursor Complex → Transition State → Product[a]

system		singlet, hartrees	ΔE_{st},[b] kcal/mol	reactant,[c] hartrees	ΔE_{int},[d] kcal/mol	ΔE_{act},[d,e] kcal/mol	ΔH,[d] kcal/mol
CpRh(CO)	MP2	−327.797 97	+5.63	−368.077 12	−13.6	−4.55 (−3.50)	−19.2
	MP4SDTQ	−414.412 67	+7.47	−454.710 37	−13.7	−3.35 (−2.77)	−11.9
CpRh(SH_2)	MP2	−225.910 34	−9.40	−266.189 50	−12.0	−6.29 (−5.12)	−24.5
	MP4SDTQ	−312.530 82	−9.52	−352.828 52	−12.2	−4.90 (−3.91)	−18.0
CpRh(PH_3)	MP2	−222.931 68	−8.17	−263.210 83	−13.0	−8.29 (−6.85)	−27.3
	MP4SDTQ	−309.560 26	−7.47	−349.857 96	−13.2	−6.99 (−5.80)	−20.0
CpIr(CO)	MP2	−325.760 92	−7.28	−366.040 07	−16.4	−10.6 (−10.3)	−32.8
	MP4SDTQ	−409.563 08	−1.06	−449.860 78	−16.4	−17.0 (−17.3)	−40.5
CpIr(SH_2)	MP2	−223.885 11	−16.6	−264.164 26	−14.9	−11.2 (−10.5)	−37.4
	MP4SDTQ	−307.666 56	−16.0	−347.964 26	−12.8	−14.2 (−13.7)	−43.8
CpIr(PH_3)	MP2	−220.907 00	−20.1	−261.186 15	−19.6	−16.3 (−15.4)	−43.1
	MP4SDTQ	−304.703 23	−20.3	−345.000 93	−14.4	−16.6 (−16.0)	−46.3

[a] At the MP2/LANL1DZ and MP4SDTQ/LANL2DZ//MP2/LANL1DZ levels, respectively. [b] The energy relative to the corresponding singlet state. The negative value means the triplet is the ground state. [c] The total energy of CH_4 at the MP2/LANL1DZ and MP4SDTQ/LANL2DZ//MP2/LANL1DZ levels of theory are −40.279 15 and −40.297 70 hartrees, respectively. [d] The energy relative to the corresponding reactants. [e] The σ attack and π attack (in parentheses) are shown here; see the text.

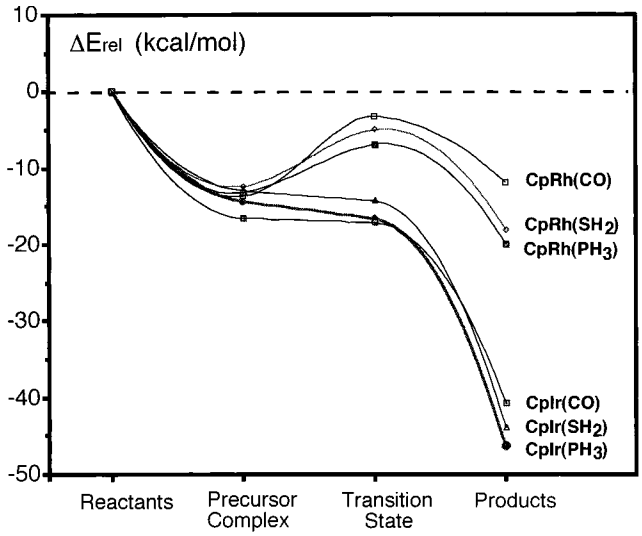

Figure 9. Potential energy profile of the reaction of CpML with CH_4. All of the energies were calculated at the MP4SDTQ/LANL2DZ//MP2/LANL1DZ level. See the text.

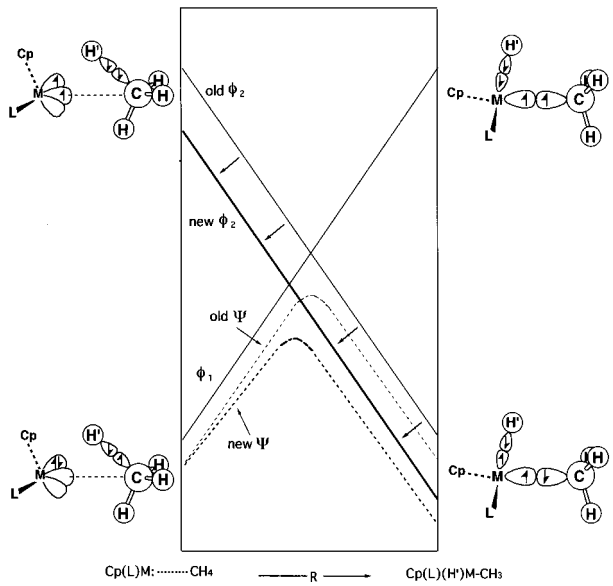

Figure 10. Energy diagram for an oxidative addition reaction showing the formation of a state curve (Ψ) by mixing two configurations: the reactant configuration (ϕ_1) and the product configuration (ϕ_2). This energy diagram also shows the effects of stabilizing the product configuration ϕ_2 (indicated by the arrows).

by the appropriate molecular orbital configuration. However, as shown in Figure 10, there are only two predominant configurations that contribute considerably to the total wave function Ψ and, in turn, affect the shape of the singlet surface. One is the reactant ground-state configuration, ϕ_1, that ends up as an excited configuration in the product region. The other is the excited configuration of the reactants, ϕ_2, that correlates with the ground state of the products. There are, of course, other intermediate configurations with different spin states that might contribute to the total wave function Ψ. But since we are only concerned with singlet states in the course of reaction, it can be assumed that those intermediate configurations contribute very little, if at all, to Ψ and can therefore be neglected. As a consequence, the reaction complex at any point on the reaction profile can be described by Ψ, a linear combination of ϕ_1 and ϕ_2, and the character of the transition state will reflect the extent of mixing between ϕ_1 and ϕ_2 in the region of the avoided crossing. It is notable that the product configuration (ϕ_2) is doubly excited with respect to the reactant configuration (ϕ_1), forms an overall singlet state, and allows both M−H and M−C bond formation and simultaneous C−H′ bond breaking. Moreover, since the barrier height is basically governed by the avoided crossing of the configuration ϕ_1 and ϕ_2, it is readily seen that $\phi_1 \rightarrow \phi_2$ excitation will correlate with the barrier, i.e., both ΔE_{st} ($=E_{triplet} - E_{singlet}$ for CpML) and $\Delta E_{\sigma\sigma^*}$ ($=E_{triplet} - E_{singlet}$ for CH_4). Accordingly, if a factor is introduced into the system which has the effect of stabilizing ϕ_2, then ϕ_2 will be displaced to a lower energy along the entire reaction coordinate (see Figure 10).[5,6] The effect of such a perturbation is predicted (1) to reduce the reaction barrier since the intended crossing of ϕ_1 and ϕ_2 is lower in energy and (2) to produce a larger exothermicity since the energy of the product is now lower than that of the reactant. It should be mentioned here that the predictions from the CM model are basically in accordance with Hammond's postulate.[25]

From the above analysis, it is easy to see that if $\Delta E_{\sigma\sigma^*}$ is a constant, then a smaller value of ΔE_{st} results in a lower barrier height and a larger exothermicity; i.e., a linear relationship between ΔE_{st} and the activation energy as well as enthalpy is expected. Our model calculations confirm this prediction. For the MP4SDTQ/LANL2DZ//MP2/LANL1DZ calculations on the aforementioned six systems, the plot of activation barrier vs ΔE_{st} is given in Figure 11: $y = 0.361x + 6.09$ ($x = \Delta E_{st}$, $y =$ the activation energy).[26] Likewise, a linear correlation between ΔE_{st} and the reaction enthalpy (y') is also obtained at the same level of theory: $y' = 1.00x - 22.3$.[27] This investigation makes it quite evident that, in order to find a good model for the facile

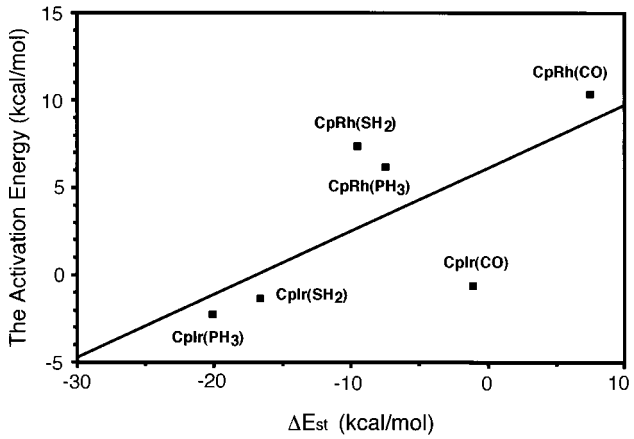

Figure 11. ΔE_{st} ($=E_{triplet} - E_{singlet}$) for CpML fragments (see the third column in Table 1) vs. the activation energy for oxidative addition of CpML fragments to methane (see the seventh column in Table 1). All were calculated at theMP4SDTQ/LANL2DZ//MP2/LANL1DZ level. See the text.

oxidative addition of 16-electron CpML to C−H bonds, an understanding of the singlet−triplet splitting ΔE_{st} of the coordinatively unsaturated CpML is very crucial.[28] Indeed, from the valence-bond point of view (right in Figure 10), the bonding in the product can be recognized as bonds formed between the triplet CpML and the two doublet radicals (overall singlet), the methyl radical and the hydrogen atom. This is much the same as the fact that the bonding in the water molecule can be viewed as bonds formed between the triplet oxygen atom and the two doublet hydrogen atoms.[4e] Accordingly, the magnitudes of the singlet−triplet splitting can be used as a basis to predict the reactivity of the reactants. If a reactant CpML has a triplet ground state or has a singlet ground state but a small excitation energy to the triplet state, then it will bring more opportunities for allowing triplet CpML to take part in the singlet reaction and can undergo single-step bond insertions. Namely, *the smaller the ΔE_{st} of CpML is, the lower the barrier height is, and in turn, the faster the oxidative addition reaction is, the larger the exothermicity is.*[28] This is exactly what we observed in the present work. We shall further discuss the substituent effect and the nature of the transition metals for such oxidative additions of CpML as follows.

Considering the substituent effect, our theoretical findings suggest that a stronger donor ligand gives a lower barrier for the oxidative addition, while a better acceptor ligand gives a lower barrier for the reductive elimination. The reason for this can be easily understood by noting the singlet−triplet splitting (ΔE_{st}) of the CpML reactant. Qualitatively, since oxidative addition involves charge transfer from the metal center of CpML to the incoming methane, an electron-donating L which can increase the electron density on the central metal would stabilize its transition state and then lower the barrier height.[29] In fact, an electron-rich metal center is recognized to be a necessary condition but not a sufficient condition for the oxidative addition of the transition-metal complexes.[1b,c,l] As a result, the more electron density on the central metal, the smaller the value of the singlet−triplet splitting ΔE_{st} and the easier the oxidative addition reaction of CpML (*vide infra*). Furthermore, since a better electron-donating group is equivalent to an ancillary ligand with lower electronegativity and a better electron-withdrawing group is a group with higher electronegativity, it is therefore reasonable to expect that the relative stabilities of the lowest singlet and triplet states should be, in turn, a sensitive function of the electronegativity of the substituents.[30] In brief summary, the reactivity of substituted 16-electron CpML is determined by its singlet−triplet splitting, which may result from electron donation or acceptance by the ancillary ligand L.

Considering the nature of the central metal, our model calculations have shown that the oxidative addition of CpIrL has a lower activation energy than that of CpRhL, while the reductive elimination of the former has a higher barrier than that of the latter. The reason for this can be traced back to the singlet−triplet splitting of CpML again. As discussed in an earlier section,[4e] since the energy required from a high-spin ground state (quartet) to a low-spin state (doublet) is much larger for the iridium atom (60.7 kcal/mol) than that for the rhodium atom (7.8 kcal/mol), one may readily conclude that the iridium system would prefer to remain on the high-spin state and, in turn, favor the triplet ground state. Conversely, the excitation energy from the high-spin state to the low-spin state for the rhodium atom is so small that the relative stability of the lowest singlet and triplet states for the CpRhL species is determined by the ancillary ligand (*vide supra*). If the ligand L is an electron-donating group, then CpRhL favors the triplet. At the other extreme, if the ligand L is an electron-withdrawing group, then CpRhL favors the singlet. These suggestions are consistent with the model calculations we present here. Indeed, it has been shown that, holding the ligands consistent, the basicity of CpIrL is higher than that of CpRhL.[31] Increasing the basicity of the metal complex can be viewed as increasing the electron density on the metal center. Such an effect, as discussed above, will reduce the singlet−triplet splitting ΔE_{st} of the CpML complex and will thus facilitate its oxidative addition reaction of alkane C−H bonds.

V. Conclusion

This work represents an attempt to apply the FMO model to explore the orientation of the organotransition-metal complex in the transition state, from which one may readily predict an approximate reaction pathway and the production of structurally distinguishable stereoisomers. Also, our work has shown that the singlet−triplet splitting ΔE_{st} ($= E_{triplet} - E_{singlet}$) based on the CM model can provide a useful basis for understanding and rationalizing the relative magnitude of the activation barriers for the oxidative addition reaction of C−H bonds to the 16-electron CpML. From the analysis in the present study, we are confident in predicting that *for the 16-electron CpML systems, a stronger electron-donating ligand (such as PMe_3, and SMe_2) and a heavier transition-metal center (i.e., the third row) will lead to a smaller ΔE_{st} and, in turn, will facilitate the oxidative addition reactions to alkane C−H bonds*. In contrast, *a better electron-withdrawing ligand (such as CO and NO^+) and a lighter transition-metal center (i.e., the second row) will result in a larger ΔE_{st} and then tend to undergo the reductive elimination reactions of forming the C−H bond*.[28] Despite the fact that the estimated magnitude of the barrier and the predicted geometry of the transition state for such reactions appear to be dependent on the calculational level applied, our qualitative predictions are in accord with the calculational results presented here as well as the available experimental observations. In spite of its simplicity, our approach can provide chemists with important insights into the factors controlling the activation of saturated C−H bonds and thus permit them to predict the reactivity of several, as yet unknown, reactive CpML intermediates.

We encourage experimentalists to carry out further experiments to confirm our predictions.

Acknowledgment. We thank the National Center for High-Performance Computing of Taiwan and the Computing Center

at Tsing Hua University for generous amounts of computing time. In addition, we thank the National Science Council of Taiwan for financial support. We thank Professor H. B. Schlegel for providing useful software. We are also grateful to referees for critical comments and helpful corrections of the manuscript.

References and Notes

(1) For reviews, see: (a) Parshall, G. W. *Acc. Chem. Res.* **1975**, *8*, 113. (b) Bergman, R. G. *Science* **1984**, *223*, 902. (c) Janowicz, A. H.; Perima, R. A.; Buchanan, J. M.; Kovac, C. A.; Struker, J. M.; Wax, M. J.; Bergman, R. G. *Pure Appl. Chem.* **1984**, *56*, 13. (d) Hill, C. L. *Activation and Functionalization of Alkanes*; Wiley: New York, 1989. (e) Halpern, J. *Inorg. Chim. Acta* **1985**, *100*, 41. (f) Ephritikhine, M. *New J. Chem.* **1986**, *10*, 9. (g) Jones, W. D.; Feher, F. J. *Acc. Chem. Res.* **1989**, *22*, 91. (h) Ryabov, A. D. *Chem. Rev.* **1990**, *90*, 403. (i) Davies, J. A.; Watson, P. L.; Liebman, J. F.; Greenberg, A. *Selective Hydrocarbon Activation, Principles and Progress*; VCH: New York, 1990. (j) Bergman, R. G. *J. Organomet. Chem.* **1990**, *400*, 273. (k) Bergman, R. G. *Adv. Chem. Ser.* **1992**, *230*, 211. (l) Wasserman, E. P.; Moore, C. B.; Bergman, R. G. *Science* **1992**, *255*, 315. (m) Crabtree, R. H. *Angew. Chem., Int. Ed. Engl.* **1993**, *32*, 789. (n) Schroder, D.; Schwarz, H. *Ibid.* **1995**, *34*, 1937. (o) Lees, A. J.; Purwoko, A. A. *Coord. Chem. Rev.* **1994**, *132*, 155. (p) Amdtsen, B. A.; Bergman, R. G.; Mobley, T. A.; Peterson, T. H. *Acc. Chem. Res.* **1995**, *28*, 154.

(2) (a) Oliver, A. J.; Graham, W. A. G. *Inorg. Chem.* **1971**, *10*, 1. (b) Janowicz, A. H.; Bergman, R. G. *J. Am. Chem. Soc.* **1982**, *104*, 352. (c) Hoyano, J. K.; Graham, W. A. G. *Ibid.* **1982**, *104*, 3723. (d) Jones, W. D.; Feher, F. *Ibid.* **1982**, *104*, 4240. (e) Janowicz, A. H.; Bergman, R. G. *Ibid.* **1983**, *105*, 3929. (f) Hoyano, J. K.; McMaster, A. D.; Graham, W. A. *Ibid.* **1983**, *105*, 7190. (g) Jones, W. D.; Feher, F. J. *Organometallics* **1983**, *2*, 562. (h) Periana, R. A.; Bergman, R. G. *J. Am. Chem. Soc.* **1984**, *106*, 7272. (i) Jones, W. D.; Feher, F. J. *Ibid.* **1984**, *106*, 1650. (j) Rest, A. J.; Whitwell, I.; Graham, W. A. G.; Hoyano, J. K.; McMaster, A. D. *J. Chem. Soc., Chem. Commun.* **1984**, 624. (k) Wax, M. J.; Stryker, J. M.; Buchanan, J. M.; Caroline, A. K.; Bergman, R. G. *J. Am. Chem. Soc.* **1984**, *106*, 1121. (l) Gilbert, T. M.; Bergman, R. G. *Ibid.* **1985**, *107*, 3502. (m) McGhee, W. D.; Bergman, R. G. *Ibid.* **1986**, *108*, 5621. (n) Haddleton, D. M. *J. Organomet. Chem.* **1986**, *311*, C21.

(3) (a) Nolan, S. P.; Hoff, C. D.; Stoutland, P. O.; Newman, L. J.; Buchanan, J. M.; Bergman, R. G.; Yang, G. K.; Peters, K. S. *J. Am. Chem. Soc.* **1987**, *109*, 3143. (b) Marx, D. E.; Lees, A. J. *Inorg. Chem.* **1988**, *27*, 1121. (c) Stoutland, P. O.; Bergman, R. G.; Nolan, S. P.; Hoff, C. D. *Polyhedron* **1988**, *7*, 1429. (d) Bloyce, P. E.; Rest, A. J.; Whitwell, I.; Graham, W. A. G.; Holmes-Smith, R. *Chem. Commun.* **1988**, 846. (e) Bell, T. W.; Haddleton, D. M.; McCamley, A.; Partridge, M. G.; Perutz, R. N.; Willner, H. *Ibid.* **1990**, *112*, 9212. (f) Barrientos, C.; Ghosh, C. K.; Graham, W. A. G.; Thomas, M. J. *J. Organomet. Chem.* **1990**, *394*, C31. (g) Weiller, B. H.; Wasserman, E. P.; Moore, C. B.; Bergman, R. G. *Ibid.* **1993**, *115*, 4326. (h) Burger, P.; Bergman, R. G. *Ibid.* **1993**, *115*, 10462. (i) Schultz, R. H.; Bengali, A. A.; Tauber, M. J.; Weiller, B. H.; Wasserman, E. P.; Kyle, K. R.; Moore, C. B.; Bergman, R. G. *Ibid.* **1994**, *116*, 7369. (j) Veltheer, J. E.; Burger, P.; Bergman, R. G. *Ibid.* **1995**, *117*, 12478. (k) Selmeczy, A. D.; Jones, W. D.; Osman, R.; Perutz, R. N. *Organometallics* **1995**, *14*, 5685. (l) Arndtsem, B. A.; Bergman, R. G. *J. Organomet. Chem.* **1995**, *504*, 143. (m) Bromberg, S. E.; Lian, T.; Bergmen, R. G.; Harris, C. B. *J. Am. Chem. Soc.* **1996**, *118*, 2069.

(4) For theoretical works, see: (a) Saillard, J.-Y.; Hoffmann, R. *J. Am. Chem. Soc.* **1984**, *106*, 2006. (b) Ziegler, T.; Tschinke, V.; Fan, L.; Becke, A. D. *Ibid.* **1989**, *111*, 9177. (c) Song, J.; Hall, M. B. *Organometallics* **1993**, *12*, 3118. (d) Musaev, D. G.; Morokuma, K. *J. Am. Chem. Soc.* **1995**, *117*, 799. (e) Siegbahn, P. E. M. *Ibid.* **1996**, *118*, 1487. (f) Jimenez-Catano, R.; Hall, M. B. *Organometallics* **1996**, *15*, 1889.

(5) Hoffmann, P.; Padmanabhan, M. *Organometallics* **1983**, *2*, 1273.

(6) Silrestre, J.; Calhorda, M. J.; Hoffman, R.; Stoutland, P. O.; Bergman, R. G. *Organometallics* **1986**, *5*, 1841.

(7) (a) Bach, R. D.; Andres, J. L.; Su, M.-D.; McDouall, J. J. W. *J. Am. Chem. Soc.* **1993**, *115*, 5768. (b) Bach, R. D.; Su, M.-D.; Aldabagh, E.; Andres, J. L.; Schlegel, H. B. *Ibid.* **1993**, *115*, 10237. (c) Bach, R. D.; Su, M.-D. *Ibid.* **1994**, *116*, 10103.

(8) (a) For a discussion, see: Jorgensen, W. L.; Salem, L. *The Organic Chemist's Book of Orbitals*; Academic: New York, 1973. (b) Meredith, C.; Hamilton, T. P.; Schaefer, H. F., III. *J. Phys. Chem.* **1992**, *96*, 9250.

(9) In this work, we shall use the σ/π nomenclature (see ref[10]) to describe the reaction trajectory and define the axis of attack of the valence orbital on the central metal.

(10) Hoffmann, R. *Angew. Chem., Int. Ed. Engl.* **1982**, *21*, 711.

(11) (a) Sosa, C.; Schlegel, H. B. *J. Am. Chem. Soc.* **1987**, *109*, 4193. (b) *Ibid.* **1987**, *109*, 7007.

(12) (a) Hay, J. P.; Wadt, W. R. *J. Chem. Phys.* **1985**, *82*, 270. (b) *Ibid.* **1985**, *82*, 284.

(13) Hay, J. P.; Wadt, W. R. *J. Chem. Phys.* **1985**, *82*, 299.

(14) For the first row atoms: Dunning, T. H.; Hay, P. J. Modern Theoretical Chemistry; Schafer, H. F., III, Ed.; Plenum: New York, 1977; p 1.

(15) For the hydrogen atom: Huzinaga, S. *J. Chem. Phys.* **1965**, *42*, 1293.

(16) Molecular orbital calculations were carried out using the Gaussian 92 program system utilizing gradient geometry optimization. Gaussian 92, Revision C: M. J. Frisch, G. W. Trucks, M. Head-Gordon, P. M. W. Gill, M. W. Wong, J. B. Foresman, B. G. Johnson, H. B. Schlegel, M. A. Robb, E. S. Replogle, R. Gomperts, J. L. Andres, K. Raghavachari, J. S. Binkley, C. Gonzalez, R. L. Martin, D. J. Fox, D. J. Defrees, J. Baker, J. J. P. Stewart, and J. A. Pople, Gaussian, Inc., Pittsburgh, PA, 1992.

(17) A similar study, sees: Su, M.-D.; Chu, S.-Y. *Organometallics*, in press.

(18) (a) Su, M.-D. *Chem. Phys. Lett.* **1995**, *237*, 317. (b) Su, M.-D. *J. Org. Chem.* **1995**, *60*, 6621. (c) Su, M.-D. *J. Phys. Chem.* **1996**, *100*, 4339. (d) Su, M.-D. *Chem. Phys.* **1996**, *205*, 277. (d) Su, M.-D. *J. Org. Chem.* **1996**, *61*, 3080.

(19) However, this prediction cannot apply to the CpCoL systems. For theoretical works, see ref 4e. For experimental works, see: (a) Rest, A. J.; Whitwell, I.; Graham, W. A. G.; Hoyano, J. K.; McMaster, A. D *J. Chem. Soc., Dalton Trans.* **1987**, 1181. (b) Janowicz, A. H.; Bryndza, H. E.; Bergman, R. G. *J. Am. Chem. Soc.* **1981**, *103*, 1516. (c) Wasserman, E. P.; Bergman, R. G.; Moore, C. B. *ibid.* **1988**, *110*, 6076. (d) Bengali, A. A.; Bergman, R. G.; Moore, C. B. *Ibid.* **1995**, *117*, 3879. Also see ref 28.

(20) It must be noted that for real ligands, of course, σ-donating power and π-accepting power are always interrelated.

(21) Cotton, F. A.; Wilkinson, G. *Advanced Inorganic Chemistry*, 3rd ed.; Wiley-Interscience: New York, 1972; pp 683−701 and references therein.

(22) Koga, N.; Morokuma, K. *J. Am. Chem. Soc.* **1993**, *115*, 6883.

(23) Su, M.-D. *Inorg. Chem.* **1995**, *34*, 3829.

(24) (a) Shaik, S.; Schlegel, H. B.; Wolfe, S. *Theoretical Aspects of Physical Organic Chemistry*; John Wiley & Sons: New York, 1992. (b) Pross, A. *Theoretical and Physical principles of Organic Reactivity*, John Wiley & Sons: New York, 1995.

(25) Hammond, G. S. *J. Am. Chem. Soc.* **1954**, *77*, 334.

(26) At the MP2/LANL1DZ level, the linear relationship is $y = 0.226x + 7.47$.

(27) At the MP2/LANL1DZ level, the linear relationship is $y' = 0.889x - 22.4$.

(28) It must be emphasized that the concept which uses the singlet−triplet splitting ΔE_{st} to predict the reactivity of the 16-electron CpML complex cannot apply to the CpCoL system. See ref 19. Indeed, Siegbahn (ref 4e) has pointed out that the cobalt atom has a high excitation energy (77.5 kcal/mol) from a quartet d^7s^2 ground state to the d^9 doublet state, implying that the CpML system has a low amount of open-shell character in the singlet state. In other words, unlike the two main configurations (ϕ_1 and ϕ_2) involved in Figure 8, in the CpCoL case, there could be three predominant configurations contributed to the total wave function Ψ, i.e., a closed-shell singlet, two open-shell triplet (so overall singlet), and an open-shell singlet. This study, however, is beyond the scope of the present work and will not be discussed here.

(29) Conversely, since reductive elimination involves the charge transfer from methane to metal, the electron-withdrawing L should stabilize the CpML compound and then allow such a reaction to proceed readily.

(30) Further work investigating the effect of the electronegativity of the ancillary ligand L on the reactivity of the CpML systems is underway.

(31) Angelici, R. J. *Acc. Chem. Res.* **1995**, *28*, 51.